

M. R. Kundu

Astronomy Program, University of Maryland, College Park, MD

I. INTRODUCTION

The centimeter -wave bursts are simple: they are characterized by a rapid rise in intensity and a slower decline. The burst-radiation is in general smooth, usually free of details in time and frequency and is a partially polarized broadband continuum. It starts almost immediately after an associated $H\alpha$ flare and originates from a source of small angular size ($< 1'$ arc). The smooth continuum emission of centimeter-wave bursts has been accounted for by synchrotron radiation from fast electrons accelerated during flares. I shall not attempt to give here a full description of the observational characteristics of centimeter bursts, rather I shall concentrate on certain specific features relevant to the understanding of the generating mechanism of these bursts. More than 20 years ago, centimeter bursts were studied with a spatial resolution as good as $\sim 1'$ arc. Even with this resolution the presence of small scale structures on scales of $1' - 4'$ were observed in $\text{cm-}\lambda$ burst sources. Since that time both spatial and time resolution have steadily improved; we now have a spatial resolution of $\gtrsim 1''$ and time resolution of ~ 10 ms. Such resolutions have revealed smaller scale structures of a few arc seconds and more complexity in burst sources. At the same time soft x-ray observations, particularly from Skylab, with resolution better than $5''$ (e.g. Kahler et al. 1975; Vorpahl et al. 1975) have given new information about the flare phenomenon. Because of the close association of soft x-ray and $\text{cm-}\lambda$ burst sources, these observations are particularly important for a proper understanding of the generating mechanism of $\text{cm-}\lambda$ bursts, acceleration of electrons and the origin of solar flares.

II. OBSERVATIONS

Flare Precursor

Observations of an active region prior to the onset of a flare are of obvious importance to our understanding of the flare build-up process. At short centimeter wavelengths (2-6 cm), one observes this flare build-up in the form of increased intensity and increased polarization of the

active region, both of which suggest that the magnetic field increases or becomes more ordered prior to the occurrence of the flare. The flare-associated bursts originate in these intense sources, and the probability of occurrence of bursts increases with the increasing intensity of these narrow bright regions (Kundu 1959). This behavior of the active region prior to the onset of flares has also been observed on spatial scales of a few arc seconds (Kundu et al. 1974; Lang 1974). Indeed, using the Owens Valley interferometer at 2.8 cm- λ with resolution of 7" arc, Lang (1974) observed circular polarization of up to 100% in the active region core (see Fig. 1). Lang (1977) also claimed that dramatic changes of up to 80% in the circular polarization of the active region core (within spatial scales of $\sim 5''$ arc) occurred approximately one hour before the flare onset. By contrast, according to Lang, no substantial variations in polarization, were observed over a quiescent period of forty hours. Since Lang's conclusions were based upon only two such cases it will be desirable to make further high resolution observations to confirm these conclusions, especially since he speculates that the pre-flare polarization changes may be related to emerging magnetic fields triggering flares.

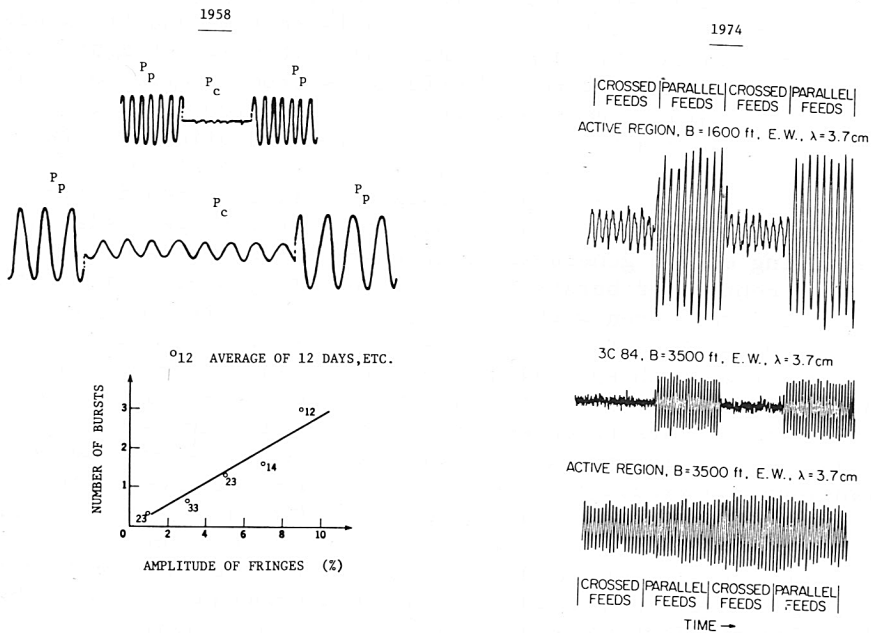


Figure 1. Top left: 3 cm solar interferometric observations with crossed and parallel feeds; Lower left: number of 3 cm- λ bursts as a function of the amplitude of fringes observed at mid-day (H.A. $\approx 0^\circ$) expressed as a percentage of the quiet sun emission (after Kundu 1959); Right: 3.7 cm interferometric observations with crossed and parallel feeds (after Lang 1974).

Recent Skylab x-ray observations have also provided evidence for

flare build-up in the form of preheating of x-ray kernels. It seems, however, that the flaring kernel is not necessarily the one that undergoes pre-heating. It should be remembered that soft x-ray pre-heating refers to 2-3 minutes before the onset of the main flare, while the radio observations refer to several hours before the onset. It is possible that the different x-ray kernels within an active region are linked by magnetic field lines as shown in Fig. 2. The kernel near one leg of the loop is likely to undergo much more pre-heating than the one on the top of the loop. According to some flare models, the kernel at the loop top will flare. This may explain why the x-ray kernel that undergoes pre-heating is not necessarily the same one that flares up. Certainly such a schematic interpretation can be tested by VLA observations with $\lesssim 1''$

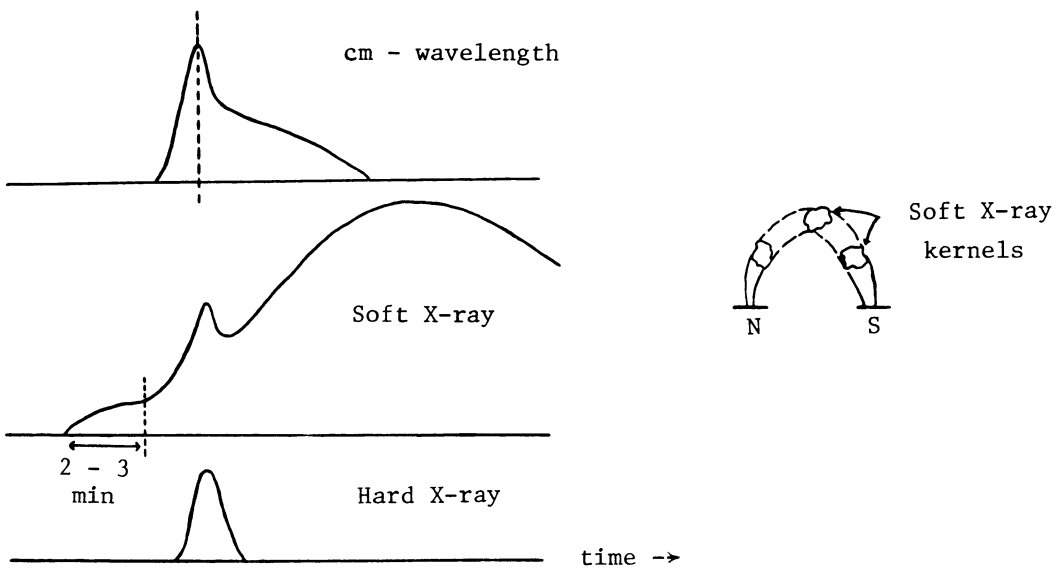


Figure 2. Left: schematic profiles showing temporal relationship between cm- λ burst, soft x-ray and hard x-ray emission; Right: schematic of a bipolar loop showing soft x-ray kernels.

resolution. Since the radio observations provide information on the magnetic field, it is of extreme importance to study the flare build-up at centimeter wavelengths with an angular resolution of $1''$ arc or less. According to the general theoretical arguments developed by Parker (1977), the magnetic fields in the active regions are continually manipulated by the convection zone and the photospheric fluid motions, the twisted components continually rise up through the surface into the apex of each re-entrant flux tube. The magnetic field lines try to reach equilibrium through reconnections, and in so doing heat the plasma or accelerate particles or both. It is entirely possible that the flare build up in the microwave domain is due to this kind of magnetic activity.

Intensity Distribution of cm- λ Bursts

The transition from the precursor stage to the "actual" burst must be a matter of definition, since the burst intensity varies from a value barely discernible above receiver noise to thousands of solar flux units. To understand the physics of energy build-up and release in flares it may be useful to study the intensity distribution of flares. Such studies have been carried out in terms of plots of number histograms of observed events against integral of peak fluxes of the events. Such plots presented for centimeter bursts (Kundu 1965), for soft x-ray bursts (Fig. 3a - Drake 1971) and for hard x-ray events (Fig. 3b - Datlowe et al. 1974) show that in each case a power-law fit for the number of events per intensity interval provides a good fit. The intensity distribution of the

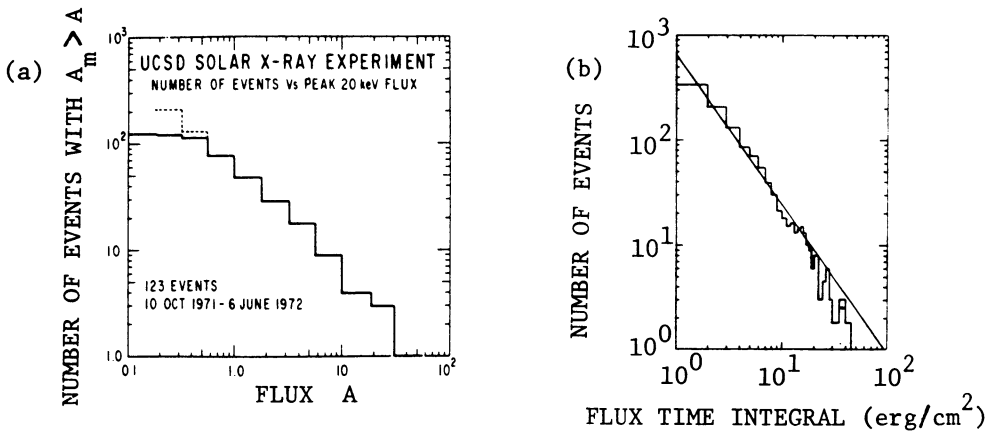


Figure 3. (a) Integral distribution of frequency of events versus hard x-ray flux. The distribution is approximately proportional to $N \sim A^{-0.8}$ for $1 \lesssim A \lesssim 10$ photons $(\text{cm}^2 \text{ s keV})^{-1}$. The dotted line represents an extrapolation of this distribution until N equals the number of soft x-ray bursts observed. If the distribution continued smoothly down to $A = 0.2$ photons $(\text{cm}^2 \text{ s keV})^{-1}$ then the ratio of hard x-ray bursts to soft x-ray bursts would be 1 (after Datlowe et al. 1974); (b) Number histogram of solar soft x-ray flare occurrence detected by Explorers 33 and 35 plotted against the total integrated flux $\int F dt$ for each event. The power law fit is characterized by an exponent 1.44 ± 0.01 (after Drake 1971).

centimeter-wavelength bursts can be represented as shown in Fig. 3c and by a curve which fits the equation $(F(I) = \Delta N / \Delta T \approx I_m^{-x}$, where $x = 1.5$ at 3 and 10 cm- λ . The term $F(I)$ is the frequency of occurrence of centimeter-wavelength bursts of mean intensity I_m , and ΔN is the number of bursts in the intensity interval ΔI . This flaring behavior at cm- λ is similar to the flaring frequency observed in soft x-rays (see Fig. 3a); Drake (1971) found that the number histograms of solar soft x-ray burst occurrence when plotted against the total integrated flux $E_T = \int F dt$ for

each event, can be fitted by a power-law with an exponent 1.44, similar to that found on cm- λ . Indeed, generalizing this flaring behavior for a variety of cosmic transient sources -- the Sun, Flare Stars (such as UV Ceti, YZ CMi - Fig. 3d) and x-ray bursters which span an energy release rate of more than 10 decades, Rosner and Vaiana (1978) showed that the frequency (ν) as a function of energy released (E) follows a similar power-law [$\nu(E) \propto E^{-X}$] at large energies for all these sources. Rosner and Vaiana (1978) tried to interpret these distributions of the flare

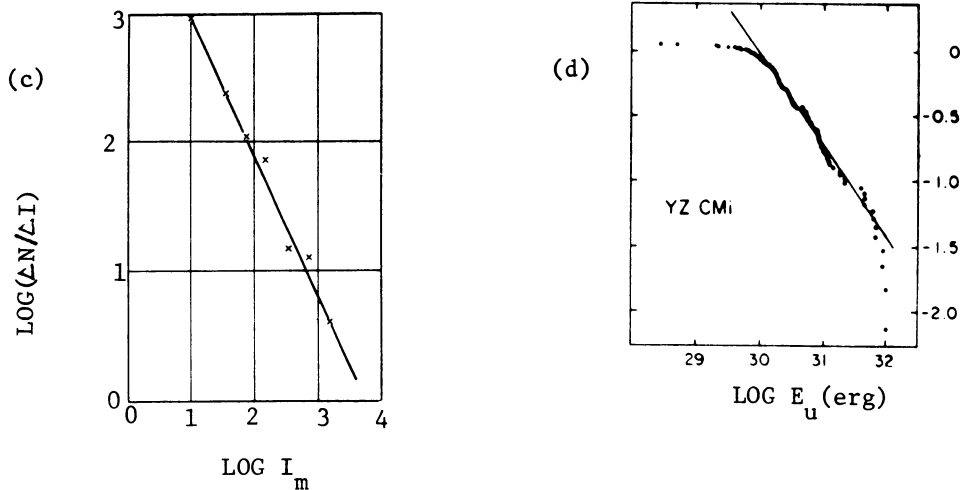


Figure 3(c) Plot of $\log(\Delta N/\Delta I)$ as a function of $\log I_m$ where $\Delta I =$ intensity interval and $\Delta N =$ Number of bursts in the interval ΔI . I_m is the mean intensity and is expressed in units of $10^{-22} \text{ w m}^{-2} \text{ Hz}^{-1}$ (after Kundu 1965). (d) Frequency histogram of optical flare occurrence from YZ CMi plotted against the total flare energy radiated in the U bandpass for each flare. The power law fit was calculated for the high energy events only and is characterized by an exponent of 21.4 ± 2 (after Lacy et al.).

energy release process, as follows: they suggested that external forces supply energy to the pre-flare volume at a rate proportional to the internal energy of the system. This suggestion is understandable in terms of Parker's (1977) theoretical arguments, that magnetic fields produced in the convecting Sun and other objects in the astrophysical universe are the cause of the activity observed in these objects. Strong magnetic fields imply vigorous photospheric fluid motions, which in return perturb and twist the emerging magnetic fields. This is related to the intuitive suggestion of Rosner and Vaiana, if we identify the internal energy of the pre-flare volume as the already emerged magnetic fields and the external forces as the convective fluid motions. Assuming that Poisson statistics governed the flare probability in time, Rosner and Vaiana derived a power-law distribution for flare energies with the exponent equal to the ratio between the mean flaring rate and the energy

build-up rate. A logical consequence of this unified description of the flaring process for diverse cosmic transients, is that the total energy released by a given flare must be related to the elapsed time since the last preceding flare, because increasing the interflare duration permits greater energy storage within the flaring volume (if the source is a single flaring region). An example was provided by the x-ray source MXB 1730-335, Fig. 3e. Similar behavior has been noted in the case of solar flares, namely, largest radio bursts occur during the decreasing or increasing phase of the solar activity cycle when there is more time available between bursts for energy to build-up.

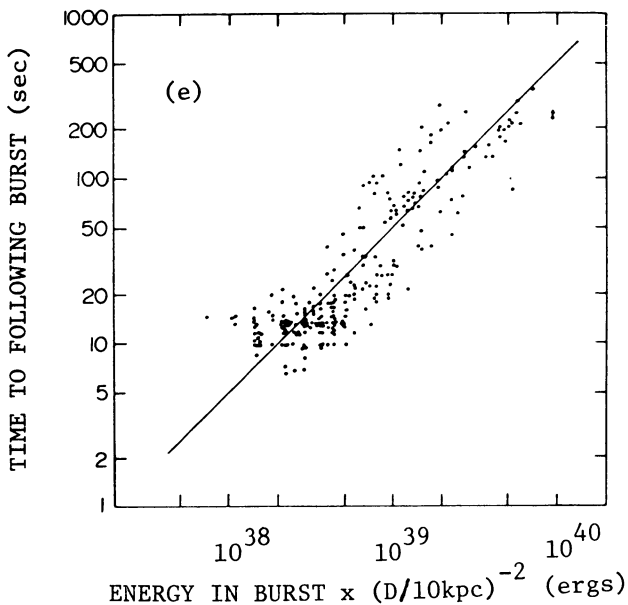


Figure 3(e). Correlation diagram of the time interval between an x-ray burst from the burster MXB 1730-335 observed by SAS-3 and the next succeeding burst and, the x-ray energy in the first burst. The burst energy ($\sim 1.5 - 10$ kev) is normalized to an assumed source distance, D , of 10 kpc. Also shown is a line indicating the expected behavior if the energy in the first burst were linearly related to the time interval between succeeding bursts (after Lewin et al. 1967).

Different Phases in cm- λ Burst Evolution

The centimeter-wave bursts are characterized by their simplicity as compared with the complex nature of the meter-wave bursts. Although the cm- λ burst is always continuum in nature, its properties, especially the spatial structure, polarization and brightness temperature change in course of the burst. Three physically significant phases in the burst emission were thus distinguished by Kundu (1959).

Impulsive Phase

The impulsive phase is characterized by a rapid rise to a peak value and a subsequent decline. It is short in duration (1 to 5 minutes). About 60 percent of these bursts are found to be partially polarized. The partial polarization is usually circular. The burst source has a diameter varying from $10''$ to $\sim 1'$ arc. The peak brightness temperatures range from 10^{10} K to about 10^8 K. This burst is caused by synchrotron radiation from nonthermal energetic electrons released and accelerated during the flare.

Post-Burst Phase

It follows a simple impulsive burst or a group of simple bursts (in the case of a complex structure). It has a duration of several minutes to about an hour. The polarization of the burst in this phase gradually decreases from that of the impulsive phase preceding it and ultimately it becomes zero. Usually its source appears to be a diffuse region of relatively large diameter ($> 1'$ arc). Its brightness temperature usually lies between 10^5 K and 10^7 K. The impulsive phase is almost always followed by the post-burst phase, although claims have been made that occasionally impulsive phase occurs in isolation. Usually these bursts are short in duration and it is difficult to separate the post-burst from the impulsive phase. Even in these cases, the decay is much slower than the rise, implying that there may, indeed, be a post-burst present. The evolution of burst size is such that for the impulsive phase the burst diameter is minimum around maximum intensity, implying that the emission region (hot and dense plasma) is very localized around maximum intensity (Fig. 4) and then gradually becomes more and more diffuse until its temperature and density become identical to those of the ambient medium (corona).

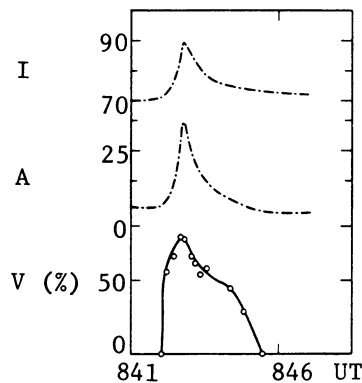


Figure 4. The evolution of a simple burst on 3 cm- λ observed on November 16, 1957. I = total intensity, A = amplitude of fringes, V = visibility of fringes. The visibility curve is simple with only one maximum (after Kundu 1959). Maximum visibility implies minimum source size.

Gradual Rise and Fall Burst

It is characterized by a slow rise to a maximum intensity and comparatively slower decline to the pre-burst level. Its duration is usually of the order of 10 minutes or longer. It is, in most cases, partially polarized, the polarization being always circular. Its source is a localized hot region of small diameter ($< 1'$ arc) with an equivalent temperature usually of the order of 10^6 K. This burst represents pre-heating of the flare plasma. The "GRF" usually occurs whenever a plasma is heated; it may occur even in the absence of a flare; for example, it occurs in association with x-ray transients that follow the disruption of filaments, without any accompanying chromospheric ($H\alpha$) flare emission (Fig. 5). The x-ray transients represent a plasma heated to temperatures of $2-3 \times 10^6$ K.

Observations with Arc-second Resolution

As discussed earlier, high resolution observations of Kundu (1959) have shown that the centimeter burst source starts with a size of slightly smaller than $1'$, condenses into a smaller region ($< 1'$ arc) and then expands to a size of $\sim 3'$ during the post-maximum decay phase. The burst is polarized mainly during the impulsive phase, the post-burst phase being essentially unpolarized. Recent high resolution interferometric observations by Hobbs et al. (1974) and Kundu et al. (1974) have provided valuable information on the existence of fine structure in the burst sources. One-dimensional fan-beam observations with a resolution of $6''$ arc at 6 cm by Alissandrakis and Kundu (1978) have proved extremely valuable; they have confirmed the polarization and spatial characteristics of microwave bursts on a scale of several arc seconds and have revealed several other interesting features. Bursts of intensity 1 to 10 sfu ($10^{-22} \text{ Wm}^{-2} \text{ Hz}^{-1}$) occur quite often near the neutral line of the magnetic field, as determined by the polarization maps of 6 cm active regions (Kundu et al. 1977). At the time of maximum (impulsive phase), the source is most compact (size $\lesssim 10''$), it is strongly polarized and the brightness temperatures generally exceed 10^8 K. After the maximum (post-burst phase), the burst core expands often with a velocity ≤ 30 km/s up to a size of $> 1'$ arc: it is unpolarized and the brightness temperature is generally $\sim 10^6$ K. At 3.7 cm, the burst source often starts with a precursor of $4''$ arc, condenses to a minimum size of $\sim 2''$ arc at the peak of the burst, after which the source expands to a size of $5''$ arc or larger. In a complex burst with several maxima, the burst sources are located at different positions; this positional change is similar to the behavior of $H\alpha$ flares which often have more than one maximum, each maximum corresponding to a small diameter "kernel" (Alissandrakis and Kundu 1975).

The 6 cm observations of Alissandrakis and Kundu (1975, 1978) with $6''$ arc resolution showed that a typical burst was polarized only in the impulsive phase and only one sense of polarization was observed near the entire extent of the burst source (Fig. 6). This suggests that, if the burst is associated with loop structures, the emission must be associated with one leg of the loop; the post-burst phase was essentially unpolar-

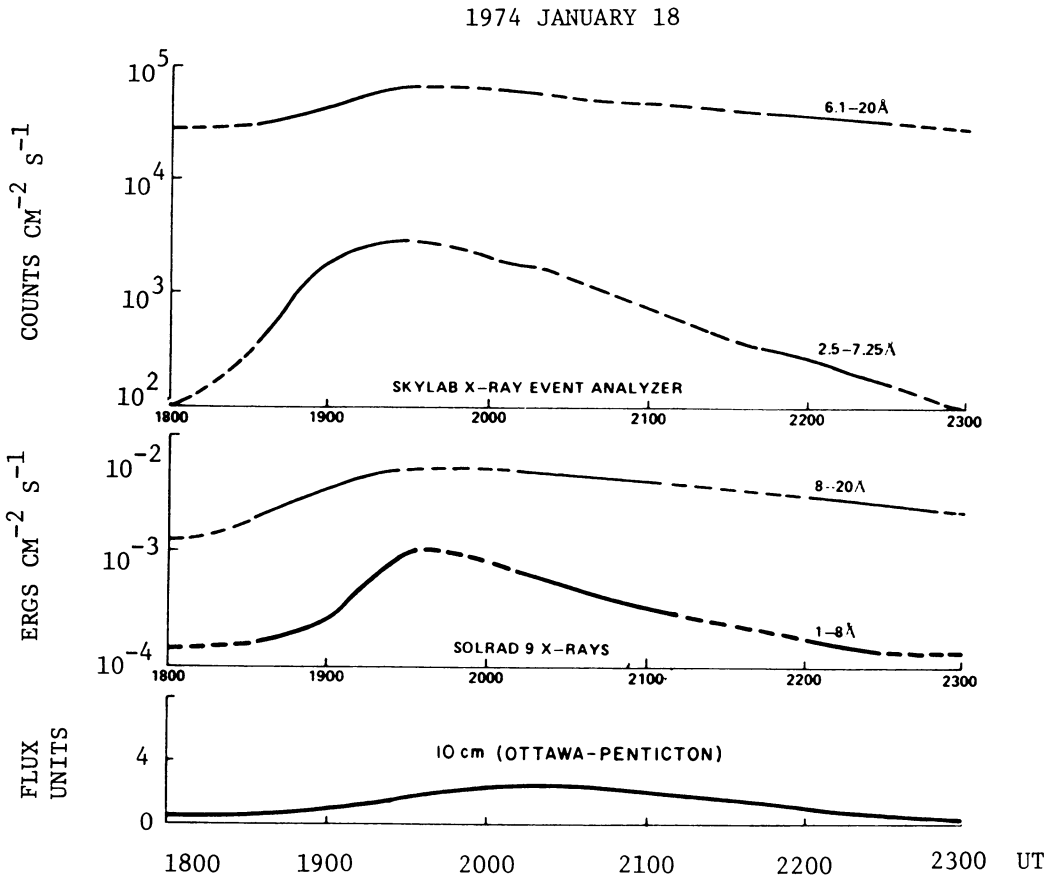


Figure 5. The time history of the integrated solar flux in the soft x-ray and microwave spectral bands illustrating the gradual-rise-and-fall (GRF) signature of a disappearing filament event. The traces shown are from the Skylab x-ray event analyzer 6.1-20 Å and 2.5-7.25 Å bands, SOLRAD-9 8-20 Å and 1.8 Å bands, and the combined Ottawa-Penticton 10-cm radio emission (after Sheely et al. 1975).

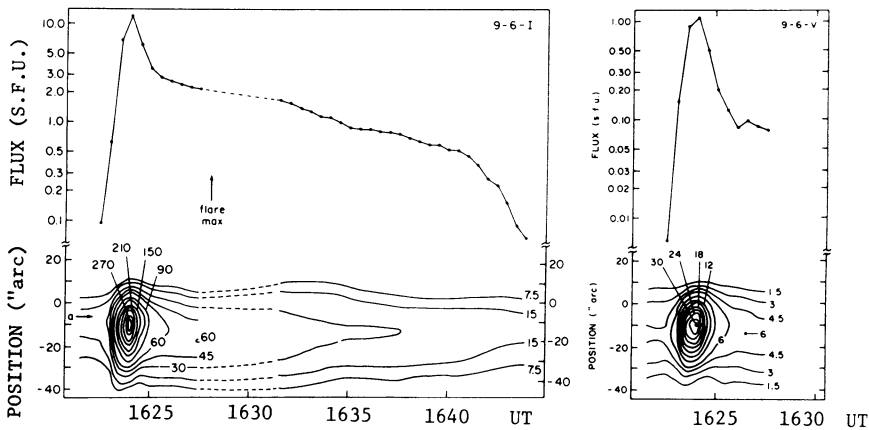


Figure 6. Total Intensity (I) and circular polarization (V) data for 6 cm burst of September 6, 1974. The upper part of the figure shows the flux in solar flux units ($10^{-22} \text{ Wm}^{-2} \text{ Hz}^{-1}$) as a function of time, while the lower part shows the one-dimensional brightness temperature as a function of position and time. Contour labels are in units of 10^6 K arcsec . Solid V-contours correspond to right-hand circular polarization (after Alissandrakis and Kundu 1978).

ized. On the other hand, Enomé et al. (1969) observed bursts of stronger intensity (~ 100 sfu) above active regions with angular resolution of $24''$. They observed both polarities (right and left circular polarization) presumably coming from opposite magnetic polarities of the loop. Qualitatively, one can explain the high resolution observations as follows. The radio spectra have a maximum at a frequency $\sim 4f_H$ ($f_H =$ gyrofrequency). For high frequencies where the source is optically thin, let us assume that the spectral index is $-\beta$. It is known that the maximum flux density for an optically thin source is proportional to NB where N is the total number of nonthermal electrons and B is the strength of the magnetic field. If the magnetic fields in the two radiation sources are of unequal strengths and the number and distribution of nonthermal electrons are equal, then the radio spectra for each of the two sources will be as sketched in Fig. 7. One can easily see from this figure that for high frequencies, e.g. at $f \gtrsim 5 \text{ GHz}$, $S_1 \gg S_2$. In fact, the ratio (S_1/S_2) is equal to $(B_1/B_2)^{1+\beta}$. Consequently, the flux density as well as the degree of polarization over the weaker pole region will be considerably reduced and sometimes, as in the case of the bursts observed by Alissandrakis and Kundu (1978), will fall below the detection limit of .05 sfu.

We consider an asymmetrical bipolar magnetic field where the two legs of the loop have dissimilar field strengths (Fig. 8). We assume that the plasma is accelerated impulsively (Brown et al. 1979) within a finite region of the loop, called the energy release region. The location of the energy release region is not critical. It can be at the top of the loop or near the stronger field leg of the loop. Electrons will flow

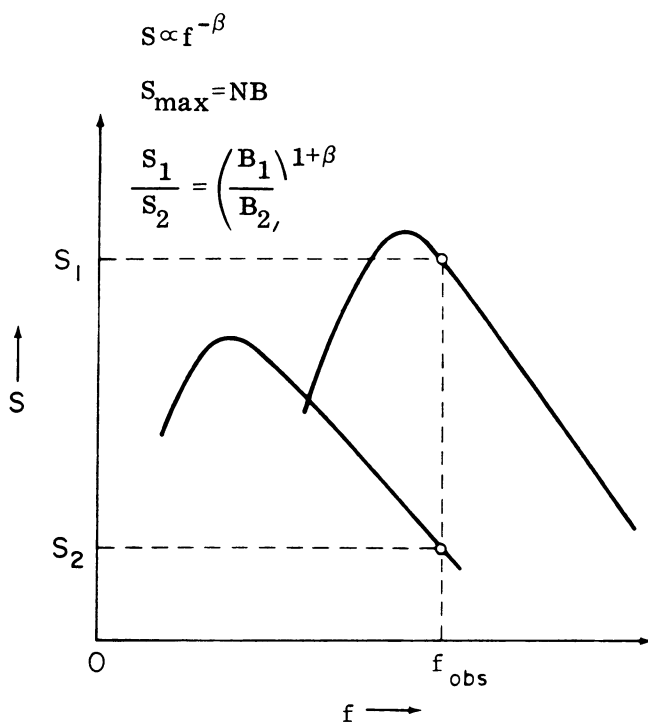


Figure 7. Schematic gyrosynchrotron radiation spectra at the two feet of an asymmetric bipolar field loop. The magnetic field strengths at the two feet are unequal ($B_1 > B_2$). S is the total flux and f is the frequency in arbitrary units (after Kundu and Vlahos 1979).

out of this region; according to Vlahos and Papadopoulos (1979) the beam of streaming particles outside the energy release region is stable. The high energy particles spread throughout the magnetic arch and produce the impulsive burst. The slower particles, in conjunction with the plasma heated by the energetic electrons, are responsible for the post-burst phase of the event. The heated plasma expands slowly along the magnetic field lines and the net effect is the filling of the loop with the hot plasma with kinetic temperature T_e . The observed characteristics of the post-burst phase can easily be explained as the radiation signature of this thermal plasma. Attempts have been made to explain the post-burst phase as due to gyrosynchrotron radiation. Among others, the main objection against this interpretation is that on the basis of synchrotron radiation one would expect the post-burst phase to be polarized and bipolar in nature. However, the observations indicate that the post-burst source is unpolarized and is of much larger size than in the impulsive phase; in fact the size in the post-burst phase is comparable to the size of the loop in which the particles are contained. We thus conclude that in the post-burst phase the bremsstrahlung emission is more dominant at the centimeter wavelengths than the gyrosynchrotron process.

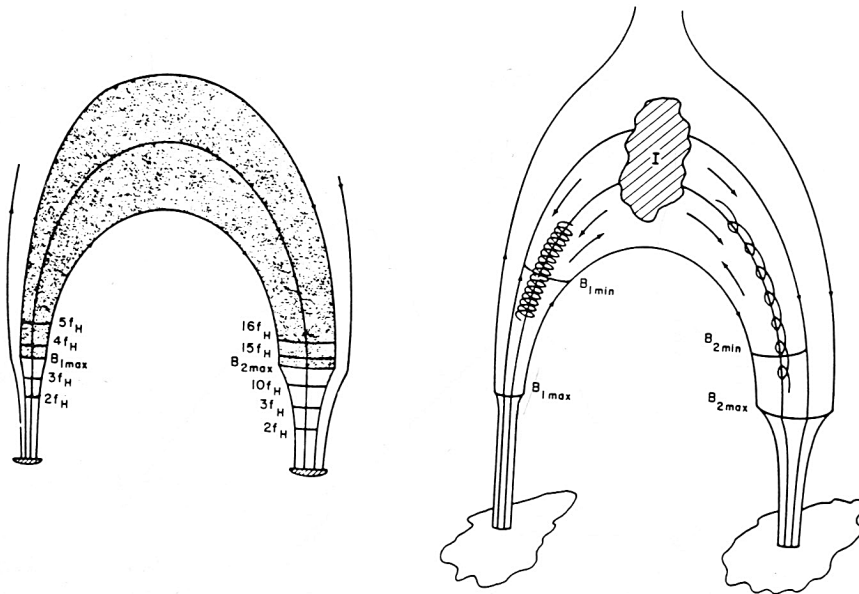


Figure 8. Right: Asymmetrical magnetic field loop above an active region; B_{\max} and B_{\min} are the maximum and minimum field strengths at each foot. Left: The gyroresonance layers for $\lambda = 6$ cm in an asymmetrical magnetic field loop. The shaded part of the loop represents the thermal plasma in the post-burst phase (after Kundu and Vlahos 1979).

Spatial Relationship of Microwave and Soft X-ray Burst Sources

For almost 20 years we have known that the impulsive cm- λ bursts have one to one correspondence with the hard x-ray bursts (> 20 keV). The cm- λ maxima always coincide almost precisely with the x-ray maxima, and there is agreement even in fine structure detail between the cm and x-ray bursts. These results have argued for a common origin for the cm- λ and hard x-ray producing electrons (Kundu 1961; DeJager and Kundu 1963).

Within the limit of uncertainties involved in the cm- λ and x-ray measurements the impulsive cm- λ bursts and the soft x-ray kernels, as measured by Skylab are found to be cospatial (Kundu et al. 1976). The source sizes in the two spectral domains are also practically the same. One of the best-studied ways of heating the flare plasma to x-ray temperatures is by collisional energy losses of 10-100 keV electrons in a thick target situation (Hudson 1973). The comparison of the spatial distribution of the nonthermal electrons as mapped by the cm- λ measurements with the soft x-ray distribution is particularly important since the soft x-ray kernels are possibly the same as the hard x-ray sources, since in a small flare the hard x-ray emission corresponds only to the impulsive phase of the associated soft x-ray burst. If the nonthermal electrons are confined to a loop and heat the soft x-ray emitting plasma by chromospheric evaporation at the loop foot points, then we should expect the cm- λ region to be no larger than the x-ray emitting region.

However, a total of about 10^{33} electrons (energy > 20 keV) is required to account for the observed intensity of some x-ray bursts. This number is higher by about two orders of magnitude than the number of electrons of several hundred keV's required to produce the centimeter-wavelength bursts by synchrotron radiation. In the past, Ramaty and Petrosian (1972) tried to resolve this discrepancy by taking into account self-absorption. On the other hand, the asymmetrical bipolar field structure as discussed earlier could also account for this discrepancy, since electrons with small pitch angles do not contribute to synchrotron radiation, but do produce bremsstrahlung bursts.

REFERENCES

- Alissandrakis, C. E. and Kundu, M. R.: 1975, *Solar Phys.* 41, 119.
 Alissandrakis, C. E. and Kundu, M. R.: 1978, *Ap. J.* 222, 342.
 Brown, J. C., Melrose, D. B. and Spicer, D. S.: 1979, *Ap. J.* 228, 592.
 Datlowe, D. W., Elcan, M. J. and Hudson, H. S.: 1974, *Solar Phys.* 39, 155.
 DeJager, C. and Kundu, M. R.: 1963, *Space Research III* (ed. W. Priester, North-Holland Publishing Co., Amsterdam-Holland), 836.
 Drake, J. F.: 1971, *Solar Phys.* 16, 152.
 Enomé, S., Kakinuma, T. and Tanaka, H.: 1969, *Solar Phys.* 6, 428.
 Hobbs, R. W., Jordan, S. D., Webster, W. J., Jr., Maran, S. P. and Caulk, H. M.: 1974, *Solar Phys.* 36, 369.
 Hudson, H. S.: 1973, *High Energy Phenomena on the Sun* (eds. Ramaty, R. and Stone, R. G.), NASA SP-342, 207.
 Kahler, S. W., Krieger, A. S. and Vaiana, G. S.: 1975, *Ap. J.* 199, L57.
 Kundu, M. R.: 1959, *Ann. d'Astrophys.* 22, 1.
 Kundu, M. R.: 1961, *J. Geophys. Res.* 66, 4308.
 Kundu, M. R.: 1965, *Solar Radio Astronomy*, Interscience, New York.
 Kundu, M. R., Velusamy, T. and Becker, R. H.: 1974, *Solar Phys.* 34, 217.
 Kundu, M. R., Alissandrakis, C. E., and Kahler, S. W.: 1976, *Solar Phys.* 50, 429.
 Kundu, M. R., Alissandrakis, C. E., Bregman, J. D., and Hin, A. C.: 1977, *Ap. J.* 213, 278.
 Kundu, M. R. and Vlahos, L.: 1979, *Ap. J.* 232, 595.
 Lacy, C. H., Moffett, T. J., and Evans, D. S.: 1976, *Ap. J. Suppl.* 30, 85.
 Lang, K. R.: 1974, *Solar Phys.* 36, 351.
 Lang, K. R.: 1977, *Solar Phys.* 52, 63.
 Lewin, W. H. G., Doty, J., Clark, G. W., Rappaport, S. A., Bradt, H. V. D., Doxsey, R., Hearn, D. R., Hoffman, J. A., Jernigen, J. G., Li, F. K., Mayer, W., McClintock, J., Primini, F. and Richardson, J.: 1976, *Ap. J.* 207, L95.
 Parker, E. N.: 1977, *Ann. Rev. Astr. Ap.* 15, 45.
 Ramaty, R. and Petrosian, V.: 1972, *Ap. J.* 178, 241.
 Rosner, R. and Vaiana, G. S.: 1978, *Ap. J.* 222, 1104.
 Sheeley, N. R., Jr., Bohlin, J. D., Brueckner, G. E., Purcell, J. D., Scherrer, V. E., Tousey, R., Smith, J. B., Jr., Speich, D. M., Tandberg-Hanssen, E., Wilson, R. M., De Loach, A. C., Hoover, R. B., McGuire, J. P.: 1975, *Solar Phys.* 45, 377.
 Vlahos, L. and Papadopoulos, K.: 1979, *Ap. J.* (in press).
 Vorpahl, J. A., Gibson, E. G., Landecker, P. B., McKenzie, D. L. and Underwood, J. H.: 1975, *Solar Phys.* 45, 199.

DISCUSSION

Benz: The observed fluctuations of the microwave background of active and quiet regions have also a power law distribution. The power law exponent is in the range from -1 to -2 . I refer to the observations reported by W. Hirth at this meeting and my own radar experiment which observed them as background. It may be taken as evidence for a similar driving force: namely magnetic energy release. In fact, there is an old suggestion of T. Gold that the relaxation of the magnetic field to a force-free configuration in upstreaming plasma is a major heat source for the corona.

Hudson: The power-law distributions for flare parameters related to total energy -- peak fluxes of microwave impulsive bursts, hard x-ray bursts, and soft x-ray bursts -- all have indices in the range 1.8-1.9. Interplanetary particles seem to have a much flatter distribution.

Kundu: I am pleased to know that even for hard x-rays the index is ~ 1.8 , I thought it was close to 1.

Stewart: You mentioned observed brightness temperatures $\sim 10^{10}$ K in impulsive microwave bursts. Such high temperatures would suggest that the emission is not due to an incoherent process, such as thermal or gyrosynchrotron radiation.

Kundu: Yes, we observed a few bursts with brightness temperatures close to 10^{10} K at 11 cm wavelength. Certainly a few times 10^9 K is not unusual.

D. Smith: When brightness temperatures of 10^{10} are observed, it is certainly necessary for some part of the radiation to be due to a coherent plasma wave emission process as for the microwave spikes observed by Slottje.

Kundu: Yes, coherent plasma radiation is a possibility. Also, gyrosynchrotron masering may provide an alternative possibility; this will be discussed by Gordon Holman in this symposium. As far as my own measurements are concerned, which have been made with a time constant of 30 or 10 second, brightness temperatures of 10^{10} K are rare, although a few times 10^9 K is quite common.

Wiehl: Did you measure any frequency dependence of the circular polarization in impulsive microwave bursts?

Kundu: With high resolution observations that I presented here of cm bursts it was not possible to measure polarization structure at more than one frequency at the same time. Of course, the polarization of total flux values of cm and dcm- λ bursts is well known; the sense of polarization seems to change from extraordinary to ordinary mode at some frequency between 2000 and 3000 MHz.

Lang: What is the degree of polarization of the small-scale ($\sim 4''$) precursor sources seen at 6 cm at Westerbork and when do they occur? Also when does the gradual build-up in circular polarization, which precedes solar impulsive events occur?

Alissandrakis: Westerbork precursor data shows a circular polarization which peaks about 30 seconds before the maximum in flare intensity.

Kundu: The degree of polarization in the precursor phase can be as high as 60–70% at 6 cm (Westerbork observations); this will occur several tens of minutes earlier than the flare.

Alissandrakis's answer regarding the circular polarization peaking 30 seconds before the burst maximum refers to the flare impulsive phase, and not to the precursor stage.